Type of article: *Original articles*

Title: Nickel-catalyzed carbonization of wood for co-production of functional carbon and fluid fuels I: production of crystallized mesoporous carbon

Authors: Tsutomu Suzuki, Kyoko Suzuki, Yukio Takahashi, Mitsuhiro Okimoto, Tetsuo Yamada, Noriyasu Okazaki, Yuichi Shimizu, Masashi Fujuwara

Names, Affiliations , Address, etc. of Authors:
Tsutomu Suzuki (Correspondent), Kyoko Suzuki, Yukio Takahashi, Mitsuhiro Okimoto, Tetsuo Yamada, Noriyasu Okazaki
Departments of Applied and Environmental Chemistry, Kitami Institute of Technology, 165 Koen-cho, Kitami, Hokkaido 090-8507, Japan
Tel. +81-157-26-9401, Fax. +81-157-24-7719
e-mail: suzuki@serv.chem.kitami-it.ac.jp

Yuichi Shimizu
Department of Science and Engineering for Materials, Tomakomai National College of Technology, 443 Nishikioka, Tomakomai, Hokkaido 059-1275, Japan
Tel. +81-144-67-8941, Fax. +81-+81-144-67-8941
e-mail: shimizu@sem.tomakomai-ct.ac.jp

Masashi Fujuwara
Graduate School of Engineering, Hokkaido University, North 13, West 8, Kita-ku, Sapporo, 060-8628 Hokkaido, Japan
Tel. +81-11-706-6568, Fax. +81-11-706-6568
e-mail: fujiwara@eng.hokudai.ac.jp

Key words:
Nickel-catalyzed carbonization, Crystallized carbon, Mesoporous structure, Dual function

Abstract

Japanese larch wood loaded with nickel (1-4 %) alone or both nickel and calcium (0.25-1.5 %) was carbonized at 800-900°C for 0-120 min with a heating rate of 5-20°Cmin^{-1} in a helium flow of 5.8-46.4 mlSTPcm^{-2}min^{-1} to examine the influence of these variables on the crystallization of carbon (the formation of T component) and the development of mesoporosity. From results obtained, reaction conditions proper to effectively produce carbon with the dual function of practically adequate electroconductivity and adsorption capacity in liquid phase were established, thereby explaining what factors would govern the process. It was also confirmed that mesoporosity developed at the cost of specific (BET) surface area in parallel with the formation of T component. This situation provided good elucidation of why the simultaneous dual function could be realized.

Introduction

Wood is a typically renewable and carbon-neutral energy resource and its conversion into liquid and gaseous fuels is recently growing in importance. Liquefaction and gasification serving the purpose have been attempted mainly in Europe and North America since the oil crisis in 1970s and to date many processes have been developed.[1,2] Current technologies are, however, still unsatisfactory in terms of commercial operation. A chief problem lies in much difficulty of complete and selective conversion into tar (oil) or gases by a single-step thermochemical process, so that the total operating cost becomes very high. This leads to the opinion that the full conversion into fluid energies is not always reasonable. On the other hand, petroleum is predicted to be exhausted about 40 years later.[3] The prediction will inform that what is expected for wood being a high quality biomass should be not only utilization as fluid fuels but also the supply of chemicals and materials as substitutes for the fossil resource.

Carbonization, which is in principle the same technology as pyrolysis,[4,5] also is a thermochemical energy conversion means in that considerable quantities of oil and gases are obtained. Although the classical technology is inferior to liquefaction and gasification in both yield and fuel quality of the corresponding product, it has industrial advantages of easier operation and lower running cost. Another important point is that the main product wood char is widely used particularly in Japan as soil improver, fodder, moisture conditioner, deodorant, etc., in addition to solid fuel. It is thus the methodological characteristic of carbonization that can afford useful functions to the solid product. Nevertheless, the potential of this technology will remain unexpanded as long as the use of wood char is limited to the present state. For raising the value of carbonization, it is needful to add new and more useful functions to the resulting char along with improvement of oil and gases in fuel quality.

From this point of view, the entitled nickel-catalyzed carbonization has been developed to report several functions for the metal-containing wood char obtained at various temperatures: (1) high gasification reactivity of 500°C-char with hydrogen[6-9], (2) good catalytic activity of chemically modified char prepared at around 600°C in hydrogenation of CO[10] and CO_2[11], and (3) practical electromagnetic shielding capacity of 900°C-char comprised of electroconductive crystallized carbon (T component).[12] Of these topics, (3) may attract the greatest attention because effective crystallization of

woody carbon at such a low temperature has never been found until then, even though nickel catalyst was used. Our recent work[13] furthermore disclosed that 900°C-char obtained from Ni 2%-loaded wood was comparable to coal-derived activated carbon[14] in the proportion of mesopore (pore with diameter of 2-50 nm) and specific surface area.[18] It follows that wood carbon having both adequate electroconductivity and adsorption capacity in liquid phase could be obtained. This is the first finding to afford simultaneously the dual function to carbon materials, thus convincing that the catalytic carbonization is an innovative method of advanced wood utilization. The aptitude of this process for improving fuel properties of liquid and gaseous fractions to be described in a subsequent paper will strengthen the conviction. However, the optimum reaction conditions, which include the loading of nickel and co-loading with calcium controlling the activity of the catalyst against the formation of T component,[15,16] to produce such a highly value-added wood carbon are not examined yet. In addition, how and why the dual function can be actualized is still uncertain. These are technologically and scientifically interesting objects deserving investigation.

Under the circumstances, the present study was conducted to examine the influence of reaction variables on the relevant properties of wood carbon obtained. As the result, suitable reaction conditions were established, thereby explaining what factors would be critical. The reason for realizing the simultaneous dual function could be elucidated as well. Discussion on these problems will lead to better understanding of this unique catalytic carbonization process of wood.

Experimental

Wood material

Powdered Japanese larch (*Larix leptolepis* GORD) with diameter of 0.50-1.40 mm was used as the raw wood material. Its ash content, determined as incombustible residue at 800°C, was 0.15%. Major metals contained were Ca, Mg, Na, K, Si, and Al, and their amounts were quantified by atomic absorption spectrometric analysis for a sample prepared by dissolving the incombustible residue with aqua regia. The compositions were 42.6, 14.9, 6.8, 11.0, 14.1, and 6.2% as CaO, MgO, Na_2O, K_2O, SiO_2, and Al_2O_3, respectively.

Nickel loading and co-loading with calcium

As the precursor of nickel, $(CH_3COO)_2Ni \cdot 4H_2O$ was loaded alone or together with $(CH_3COO)_2Ca \cdot H_2O$ onto raw wood by usual aqueous impregnation.[6-9,12] Loadings of nickel and calcium were adjusted to 1, 2, and 4% and 0.25, 0.50, 1.0, and 1.5 % as metal in wood, respectively. After impregnation, excess water was removed in a rotary evaporator at reduced pressure (20-30kPa, 30-40°C). The loading of nickel alone and co-loadings of nickel and calcium are thereafter written as 'Ni-' and 'Ni+Ca-', respectively.

Carbonization

The reaction apparatus used in this experiment is schematically shown in Fig. 1. About 2 g of Ni- or Ni+Ca-wood was packed in a stainless vessel and the vessel was placed in a vertical quartz tube reactor. The reactor was then electrically heated at a rate of 5-20°Cmin^{-1} in a helium flow of 5.8-46.4 mlSTP$cm^{-2}min^{-1}$ to a desired temperature (800-900°C) and the temperature was maintained for 0-120 min. The same treatment was made with raw (None-) wood as reference. Liquid and gaseous fractions produced during the carbonization were condensed in cold traps and collected in sampling bags, respectively, to analyze the composition, as will be described elsewhere. For reaction variables, unless otherwise noted, carbonization temperature, holding time, helium flow, and heating rate were 900°C, 60 min, 23.2 mlSTP$cm^{-2}min^{-1}$, and 10°Cmin^{-1}, respectively.

Crystal structure of carbon, surface area, and pore structure

After weighing to obtain yield on an ash-free, additives-free basis, the resulting char was subjected to measurements of X-ray diffraction (XRD, Rigaku RINT 1200) and adsorption and desorption isotherms of nitrogen at 77 K (ThermoQuest Sorptomatic 1990). In XRD, Cu-Kα ray was radiated to calculate the average crystallite size of carbon indicating to the thickness of the hexagonal layer, *Lc*, and the spacing of the plane, *d*002, from the profile. Peak intensity at (002) plane was given relative to that of artificial graphite Lonza and the value expressed as RPI was also employed as a parameter of carbon crystallization. In judgment of the crystallization, practical

standard in terms of electromagnetic shielding capacity, 8.5 nm and 15 x 10^{-3} for Lc and RPI, respectively,[13] was adopted. For nitrogen isotherms obtained, BET[17] and BJH[18] methods were applied to determine BET surface area (SBET), BJH mesopore surface area (Sm), BJH mesopore volume (Vm), and BJH total pore volume (Vt). Volumes occupied by micropore (pore with diameter of < 2 nm) and macropore (the diameter > 50 nm) also were obtained by BJH method and they are denoted as Vi and Va, respectively (Vi + Vm + Va = Vt). Parameters employed for evaluating mesoporosity were Sm and Vm, and their standards were settled on 140 m^2g^{-1} and 0.17 cm^3g^{-1}, respectively, by assuming the application of mesoporous carbon obtained to liquid phase adsorption of macromolecules.[19,20] In addition, Rv, which is defined as the ratio of Vm to Vt, was used to check the selectivity of mesopore as before.[13]

Results

Influence of carbonization temperature and nickel loading

Figure 2 illustrates XRD profiles of 800-, 850-, and 900°C-chars obtained from Ni 1%, 2%-, and 4% woods. As already stated for Ni 2%-wood,[13] the formation of T component that can be verified by a relatively sharp line at 26° was a little more effective at 900°C than at 850°C and insufficient at 800°C. A quite similar situation was found for Ni 1% and 4% and thus the three loadings of nickel gave little difference in the peak intensity at each temperature. In this figure, two sharp peaks due to metallic nickel appeared at 44 and 51° for all of Ni-chars and their intensities depended upon nickel loading, as is usual. A small peak at about 42° is assigned to another carbon crystallite corresponding to the width of the layer and its intensity was approximately proportional to that of the peak at 26°. Figure 3 represents (A) isotherms of nitrogen adsorption and desorption for the same set of chars as (B) in Fig. 1 and (B) those of 900°C-chars from three Ni-woods. As is seen for Fig. 3(A), a gap between the two curves at about 0.5-0.9 of P/P_0 was wider for higher temperature, implying an increased proportion of mesopore by increasing the temperature, although 850- and 900°C-chars did not differ greatly. These features analogous to those of the above-mentioned crystallization of carbon were likewise observed for the isotherms of Ni 1% and 4%. That is, difference in mesoporosity among the three Ni-chars was small when the temperature was identical, as can be estimated from Fig. 3(B). Table

1 summarizes properties relating to crystal structure and pore structure of carbon together with char yield for all of Ni-chars, as well as None-chars. Besides the production of amorphous carbon having a small proportion of mesopore by none-loading at any temperature, the followings are affirmed from the data of Ni-chars: (1) 800°C was too low for attaining the above-mentioned standards of *Lc*, RPI, Sm, and Vm, (2) 900°C surpassed 850°C in all the values of four parameters to exceed their standards irrespective of nickel loading, (3) Ni 2% gave larger RPI and Sm than Ni 1% and 4% at 900°C, though smaller in Rv. On the grounds of (1), (2), and (3), 900°C and Ni 2% were decided to be proper as the temperature and the loading, respectively, for producing crystallized mesoporous carbon. For char yield, it tended to increase with increasing the loading of nickel in agreement with our previous result,[12] although it is free from discussion in this study.

Influence of calcium co-loading

According to the decision in the preceding section, 900°C and Ni 2% were chosen to deal with this subject. For comparison, 850°C-carbonization with the same nickel loading was done. Figure 4 displays (A) changes of RPI and Vm and (B) those of S_{BET} and Sm with calcium co-loading, respectively, for chars obtained. At both temperatures RPI and Vm decreased in a nearly identical pattern with increasing the amount of calcium. The change of Sm was similar to those of RPI and Vm, whereas that of S_{BET} was opposite. Thus co-loading of calcium helped to increase S_{BET}, thereby retarding the crystallization of carbon and the development of mesoporosity. This revealed the unfavorable effect of foreign calcium on both formation of T component and mesopore for wood carbon, although the disadvantage was less serious for 900°C-carbonization.

Influence of helium flow, heating rate, and holding time

Table 2 lists data of 900°C-carbonization with Ni 2% to show the influence of entitled reaction variables. At four different helium flows tested, all of *Lc*, RPI, Sm, and Vm satisfied their standards. However, values of these parameters at 11.6 and 23.2 ml were larger than those at 5.8 and 46.4 ml. The suitableness of 11.6-23.2 ml was also recognized for 850°C and Ni 1 and 4%. Variation of heating rate from 5 to

20°Cmin^{-1} made no serious difference in the crystal and mesoporous structure of carbon, and satisfactory results were obtained at all three rates. The change of this variable was likewise trivial for other samples, and 10°Cmin^{-1} was proper enough. Holding time had a great influence particularly in the initial period up to 60 min, as was common to all carbonizations. For this reaction system, prolonging from 90 to 120 min induced the transition of mesopore to macropore to some extent with a little increase of RPI and a small decrease of SBET. A similar change with a loss of mesopore in this period was found for other systems. The growth into macropore was thus unimportant for the crystallization of carbon, and Sm and Vm, as well as *Lc* and RPI, usually reached their maximums at 60 to 90min.

Relationship between the crystallization of carbon and the development of mesopore

Figure 5 presents plots of SBET, Sm, and Vm against PRI, in which all of data given in Tables 1 and 2 and Fig. 4 are included and they are distinguished by open and closed symbols for nickel loading alone and co-loading with calcium, respectively. As can be foreseen from each table and figure, Sm, Vm, and SBET tended to increase for the former two and decrease for the latter with increasing PRI, although the aspect appeared to be somewhat different for the absence and the presence of foreign calcium. As a matter of course, the tendency was unchanged when RPI was replaced by *Lc*. It is thus confirmed that the development of mesoporosity had a close relationship with the crystallization of carbon, thereby simultaneously realizing the dual functional wood carbon. It becomes also evident that the increase of mesopre accompanied the decrease of SBET.

Discussion

The foregoing results demonstrated effective production of crystallized mesoporous carbon achieved by the following combination of reaction variables: loading of 2% nickel without calcium, treatment at 900°C for 60-90 min, helium flow of 11.6-23.2 mlSTPcm^{-2}min^{-1}, and heating rate of 10°Cmin^{-1}. They also reconfirmed a close correlationship between the crystallization of carbon and the development of mesopore. It is more significant from technological and scientifical points of view to clarify what factors would govern the reaction process and how and why the high correlation was

found for carbon crystallization and mesoporosity. Discussion was thus focused on these problems to refer to features of the catalytic carbonization with nickel.

As expected, carbonization temperature was a foremost factor actualizing the dual function of wood carbon simultaneously. It is ascertained by so strong domination over the activity of nickel as to become effective at 850 and 900°C independent of the loading (Figs. 2 and 3, and Table 1). This pointed out that 850°C would approximate the lower limit for making the catalysis practically available, although 900°C was more favorable. It is to be emphasized again that even 900°C is a much lower temperature for crystallizing wood carbon compared to literature.[21,22] Needless to say, the low temperature carbonization can be successfully accomplished by the aid of catalytically active nickel. Thus nickel loading is usually a critical factor, but difference in four parameters for Ni 1%, 2%, and 4% was rather small (Table 1). It would be the reason that Ni 1% exerted an almost satisfactory effect and Ni 4% was too much for loading. The percentage of 1, 2, and 4% for wood amounted to about 4, 8, and 15% respectively, in the resulting char when considering the yield (Table 1). Therefore Ni 1% was by no means a small loading, but without high dispersion of the metal precursor particles within wood tissue, desirable activity cannot be acquired.[12] Excess loading of catalyst, corresponding to Ni 4%, in general brings on worse dispersion, so that the effect often enhances to a smaller degree than expectation or sometimes lessens inversely. Another possibility for Ni 4 % inferior to Ni 2% particularly in the effect on the crystallization of carbon is degradation of the crystal structure by accelerated gasification.[16] By these explanation the proper loading of the catalyst can be understood. Although a clear difference may be seen for less the loading than 1%, the confirmation is out of the purpose of this study. It was unexpected that any co-loading of calcium diminished RPI (Fig. 4(A)), since its optimum amount for the formation of T component was previously observed for lignin-based char.[16] However, this is not necessarily incomprehensible with wood char. The earlier finding that inherent mineral matter in wood (0.15%) could act adequately as the promoter for nickel catalyst[15] suggests that even 0.25% addition of foreign calcium was excessive. The presence of calcium was coincidently unfavorable for Sm and Vm (Fig. 4). This inconvenience was, however, so valuable as to corroborate that the production of crystallized carbon and the development of mesoporosity took place at the cost of S_{BET} in concurrence with each other (Fig. 5), although co-loading with calcium is not always equivalent to diminishment of nickel loading in the catalytic mechanism. For

the decrease of S_{BET}, it is interpreted as the result of coalescence of micropore into mesopore by taking the relation with Sm and Vm into consideration. In fact, this interpretation does not contradict either theory of BET[21] and BJH.[22] Because the crystallite size of T component is in the order of 10 nm consistent to the diameter of mesopore, the formation of the crystallized carbon will involve the structural change by which mesoporosity can be enhanced. It will be thus inevitable as well that the crystallization of carbon makes S_{BET} decrease. These statements can be accepted as a persuasive reason for the close interrelationship among S_{BET}, Sm-Vm, and *Lc*-RPI (Fig. 5). The only exception in terms of the relationship between S_{BET} and Sm-Vm was the decrease of these values by extending the time from 90 to 120 min (Table 2). This occasion can be, however, accounted for by the loss of mesopore once generated from micropore to transform into macropore. Concerning helium flow, appearance of the optimal value implied that diffusive migration and/or deposition of carbon species on nickel catalyst[23] was an important step for crystallizing carbon and so developing mesoporous structure. That is, 46.4 $mlcm^{-2}min^{-1}$ was too large to promote the diffusion and/or deposition step (Table 2). However, when the flow was in the proper zone (11.6-23.2 $mlcm^{-2}min^{-1}$), this variable had a limited influence. This was also the case with the heating rate. Correctly speaking, the heating rate so varied in a moderate range that it became much less important than carbonization temperature and nickel loading as the factor. Nevertheless, adoption of the rate without great difference from that used in conventional wood carbonization has a technologically great importance in that it guarantees the easy and simple operation of the nickel-catalyzed carbonization. As for the influence of holding time, it is interesting that a part of mesopore was changed into macropore in the latter period of 90-120 min. Although the long latent period for the transition will probably reflect difficult formation of macropore, whether the difficulty is attributed to the activity loss of nickel or low thermal conductivity of carbon remains undecided at the present stage. Further investigation with different approach may be required for explaining fully this problem.

Conclusions

Nickel-catalyzed carbonization of larch wood was conducted to examine the influence of reaction variable on the crystallization of carbon (the formation of T component)

and the development of mesopore. As the result, proper conditions were established to effectively produce crystallized mesoporous carbon with electroconductivity and adsorption capacity in liquid phase. In this connection carbonization temperature was found to be a foremost factor governing the reaction process. It was also confirmed that development of mesoporosity took place at the cost of BET surface area in parallel with the crystallization of carbon. The close interrelationship for BET surface area, mesoporosity, and crystallized carbon will explain how and why the dual function could be actualized simultaneously.

Ackowledgments

This work was supported by a Grant-in Aid for Scientific Research (14560128) from the Ministry of Education, Culture, Sports, Science and Technology, Japan.

References

1. Bridgwater A V, Czenik S, Piskortz J (2001) An overview of fast pyrolysis. In: Progress in Thermochemical Biomass Conversion, Bridgwater A V (ed), BlackwellScience, Oxford, pp. 977-997
2. Maniatis K (2001) Progress in biomass gasification: an overview. In: Progress in Thermochemical Biomass Conversion, Bridgwater A V (ed), Blackwell Science, Oxford, pp. 1-31
3. Suzuki T (2000) Catalyst technology used in biomass conversion into liquid and gaseous fuels (in Japanese). Shokubai 42:521-525
4. Bridgwater A V, Bridge S (1991) A review of biomass pyrolysis and pyrolysis technologies. In: Biomass pyrolysis liquids upgrading and utilization, Bridgwater A V, Grassi G (ed), Elsevier Applied Science, London, pp. 11-92
5. Elliott D C, Beckman D, Bridgwater A V, Diebold J P, Gevert S B, Solantausta Y (1991) Developments in direct thermochemical liquefaction of biomass: 1983-1990. Energy Fuels 5:399-410
6. Suzuki T, Yamada T, Homma T (1985) Hydrogasification of wood for high heating-value gas production II.-Influence of the method of catalyst addition and gasification temperature on the CH_4 production (in Japanese). Mokuzai gakkaishi 31:595-602
7. Suzuki T, Yamada T, Homma T (1992) Hydrogasification of wood for high heating-value gas production VII-Different low temperaure hydrogasification reactivities between wood and bark chars loaded with nickel and iron catalysts. Mokuzai gakkaishi 38:509-515
8. Suzuki T, Minami H, Yamada T, Homma T (1994) Catalytic activities of ion-exchanged nickel and iron on low temperature hydrogasification of raw and modified birch chars. Fuel 73:1836-1841
9. Suzuki T, Iwasaki J, Tanaka K, Okazaki N, Funaki M, Yamada T (1998) Influence of calcium on the catalytic behavior of nickel in low temperature hydrogasification of wood char. Fuel 77:763-767
10. Suzuki T, Imizu Y, Satoh Y, Ozaki S (1995) High catalytic activity of ion-exchanged nickel on carboxymethylated wood char in methanation of carbon monoxide. Chem Letters No. 8:699-700
11. Suzuki T (2003) Nickel-catalyzed carbonization of wood for conversion to energy

and material (in Japanese). Research J Food Agric 26(6):20-25
12. Suzuki T, Yamada T, Okazaki N, Tada A, Nakanishi M, Futamata M, Chen H T (2001) Electromagnetic shielding capacity of wood char loaded with nickel. Materials Sci Res International 7:206-212
13. Suzuki K, Suzuki T, Takahashi Y, Okimoto M, Yamada T, Okazaki N, Shimizu Y, Fujuwara M (2005) Preparation of crystallized and mesoporous carbon by nickel-catalyzed carbonization of wood. Chem Letters 34:870-871
14. Yoshizawa N, Yamada Y, Furuta T, Shiraishi M, Kojima S, Tamai H, Yasuda H (1997) Coal-based activated carbons prepared with organometallics and their mesoporous structure. Energy Fuels 11:327-330
15. Wang X S, Okazaki N, Suzuki T, Funaoka M (2003) Effect of calcium on the catalysis of nickel in the production of crystallized carbon from lignocresol for electromagnetic shielding. Chem Letters 32:42-43
16. Wang X S, Suzuki T, Funaoka M (2004) Production of crystallized carbon for electromagnetic shielding from lignocresol by nickel-catalyzed carbonization-Influence of calcium co-loading (I). Materials Sci Res International 10:48-52
17. Brunauer S, Emmett P H, Teller E (1938) Adsorption of gases in multimolecular layers. J Am Chem Soc 60:309-319
18. Barrett E P, Joyner L G, Halenda P P (1951) The determination of pore volume and area distributions in porous substances I. Computations from nitrogen isotherms., J Am Chem Soc 73:373-380
19. Fitzer E (1987) The future of carbon-carbon composites. Carbon 25:163-190
20. Nishimiya K, Hata T, Imamura Y, Ishihara S (1998) Analysis of chemical structure of wood charcoal by X-ray photoelectron spectroscopy. J Wood Sci 44:56-61
21. Yasuda H, Tamai H (1996) New porous carbon materials and their adsorption characteristics (in Japanese). Kagakukogyo No.4:37-43
22. Tamai H, Kakii T, Hirota Y, Kumamoto T, Yasuda H (1996) Synthesis of extremely large mesoporous activated carbon and its unique adsorption for giant molecules. Chem Mater 8:454-462
23. Shiraishi M (1984) Graphitization of carbon (in Japanese). In: An Introduction to Carbon Materials, Inagaki M (ed), Carbon Society of Japan, Tokyo, pp. 29-40

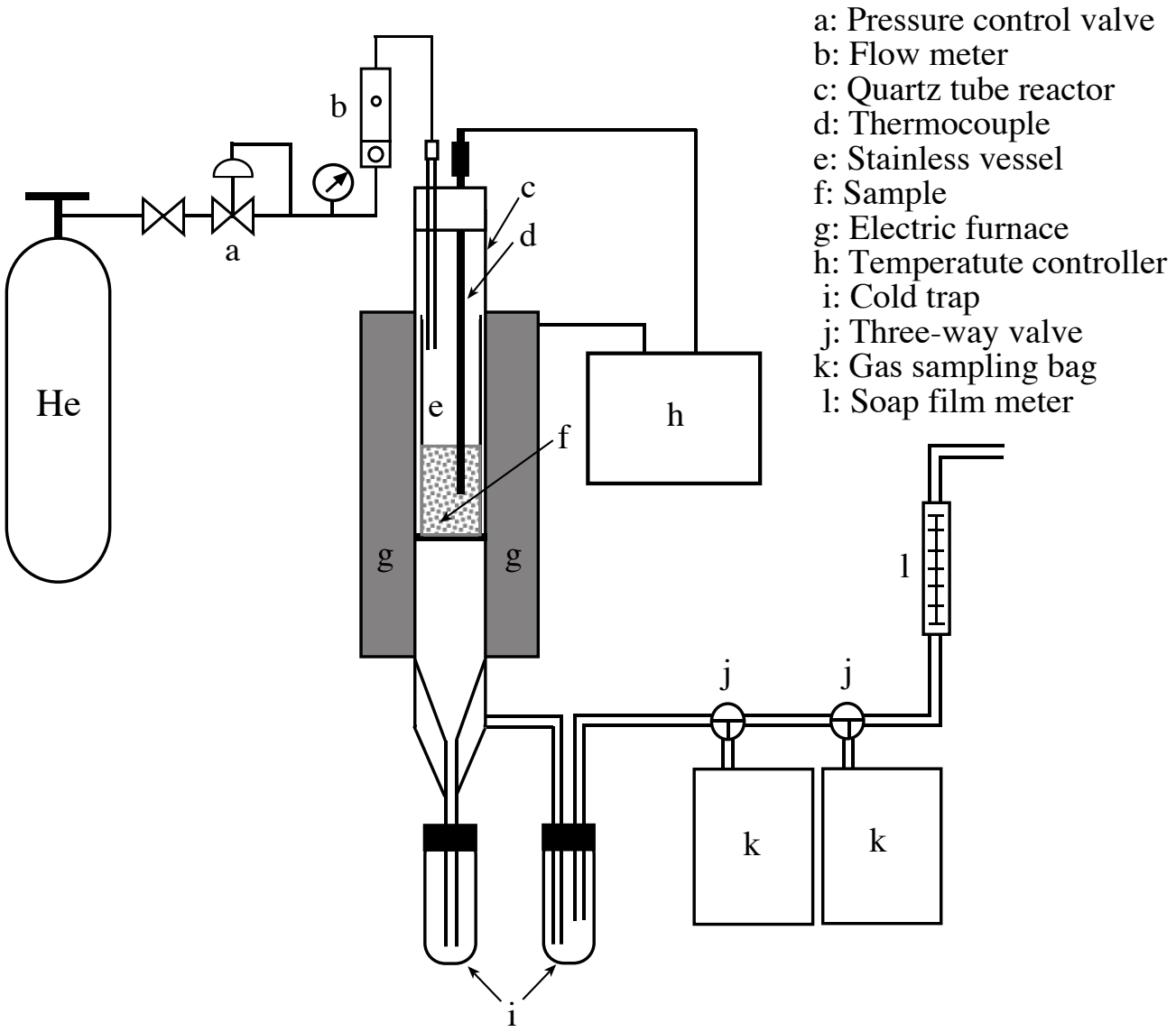
a: Pressure control valve
b: Flow meter
c: Quartz tube reactor
d: Thermocouple
e: Stainless vessel
f: Sample
g: Electric furnace
h: Temperatute controller
i: Cold trap
j: Three-way valve
k: Gas sampling bag
l: Soap film meter
He
a
b
c
d
e
f
g
g
h
i
j
j
k
k
l

Fig. 1.

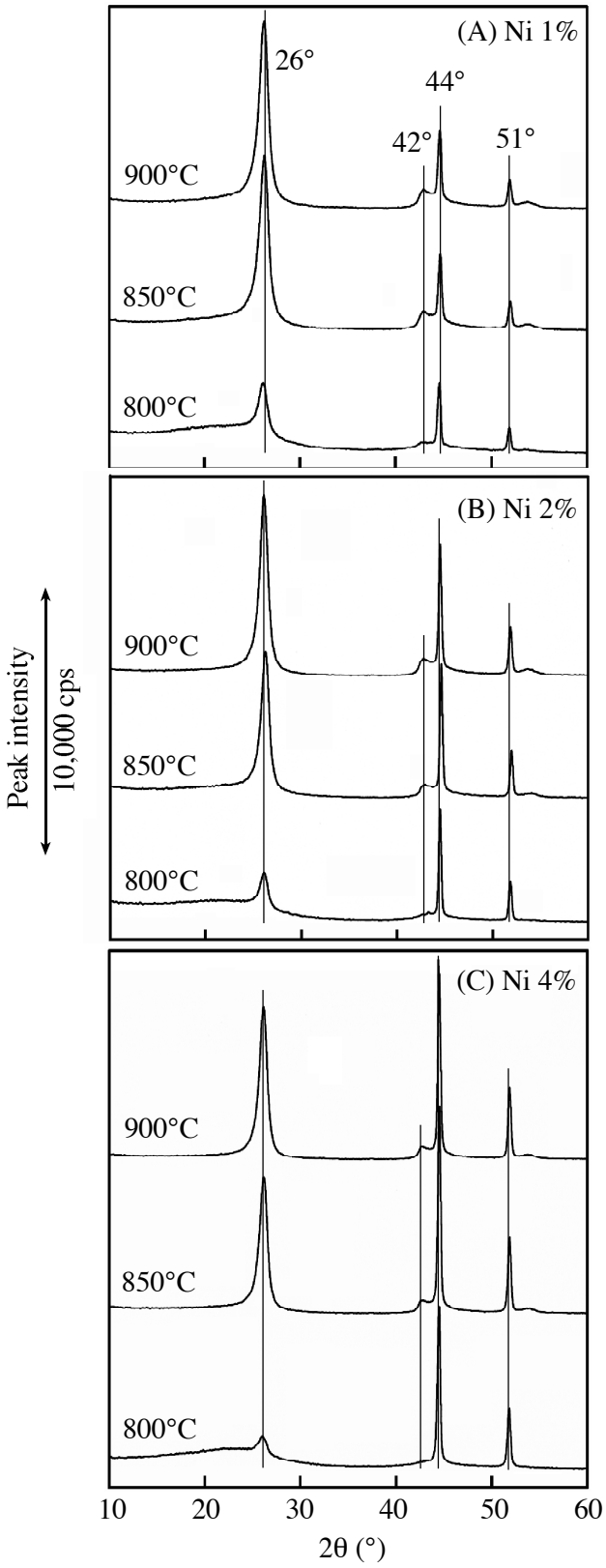
(A) Ni 1%
26°
44°
42°
51°
900°C
850°C
800°C
(B) Ni 2%
900°C
850°C
800°C
(C) Ni 4%
900°C
850°C
800°C
Peak intensity
10,000 cps
10
20
30
40
50
60
2θ (°)

Fig. 2.

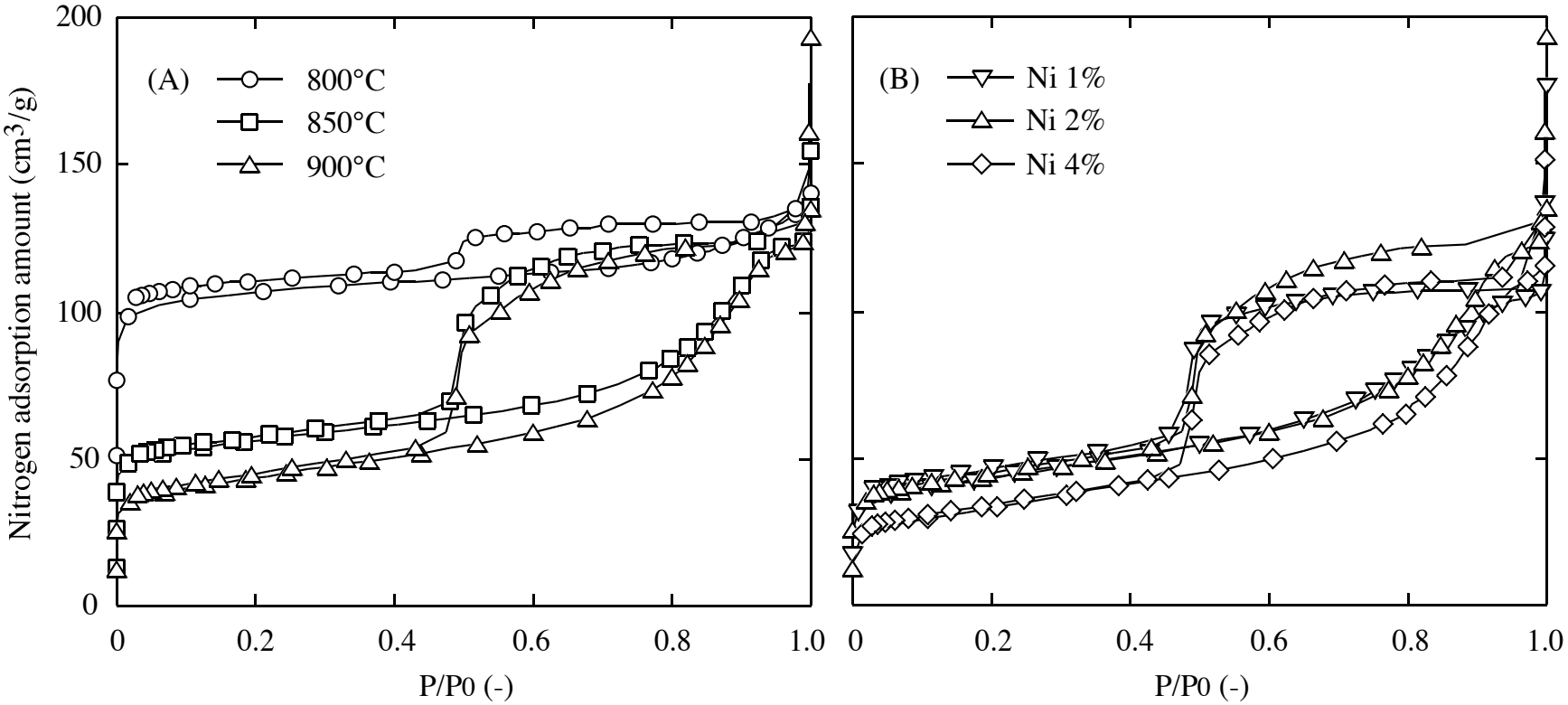
(A)
800°C
850°C
900°C
(B)
Ni 1%
Ni 2%
Ni 4%
Nitrogen adsorption amount (cm3/g)
P/P0 (-)
P/P0 (-)
0
50
100
150
200
0
0.2
0.4
0.6
0.8
1.0

Fig. 3.

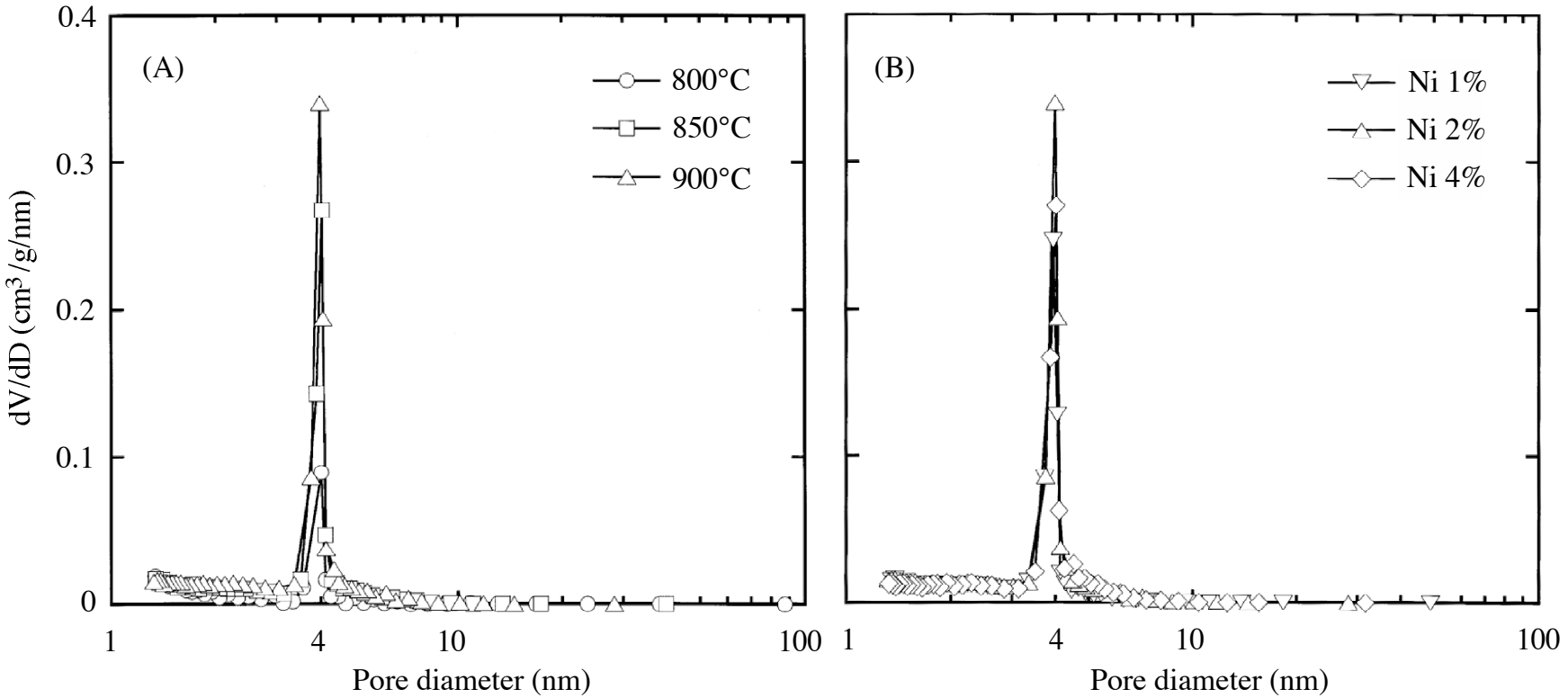
(A)
800°C
850°C
900°C
dV/dD (cm³/g/nm)
0.4
0.3
0.2
0.1
0
1
4
10
100
Pore diameter (nm)
(B)
Ni 1%
Ni 2%
Ni 4%
1
4
10
100
Pore diameter (nm)

Fig. 4.

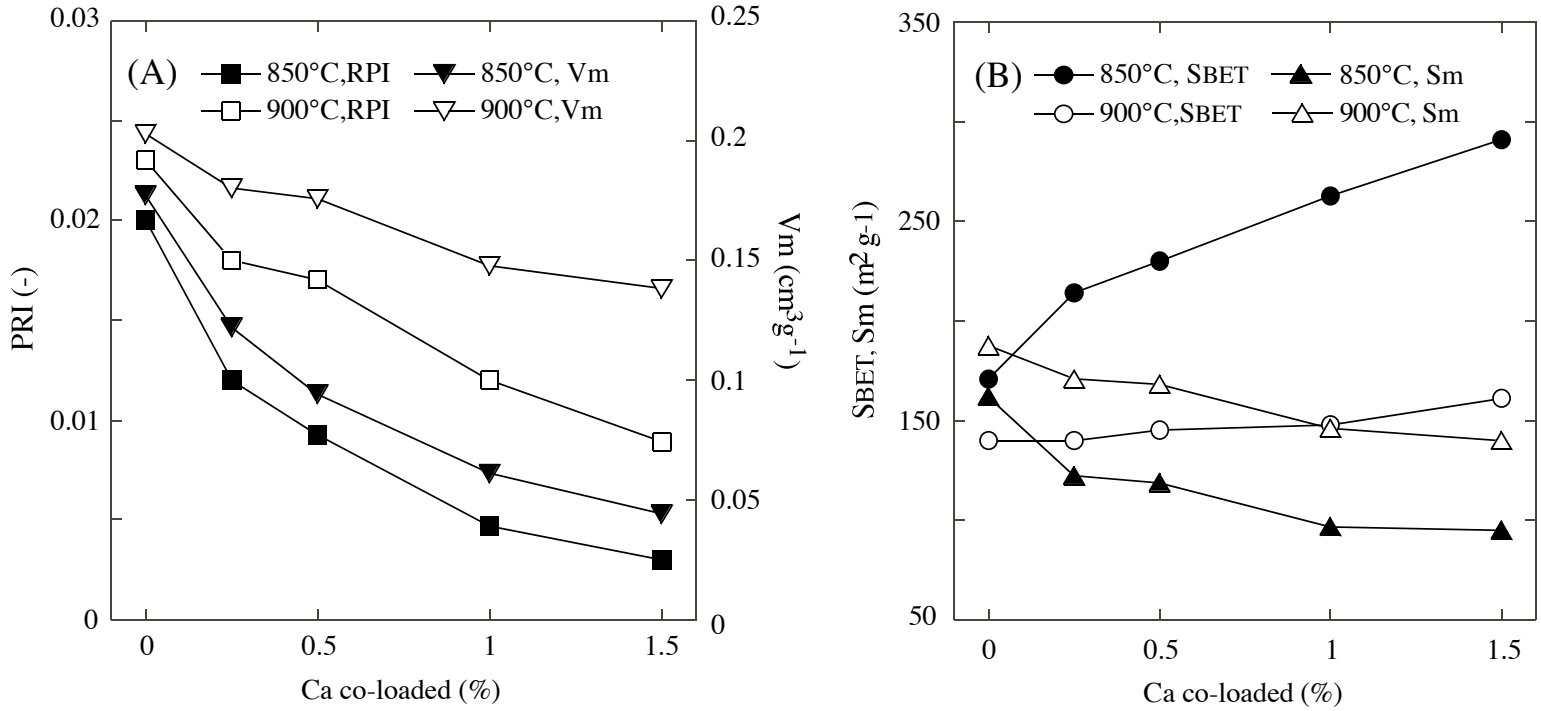
(A)
850°C,RPI
850°C, Vm
900°C,RPI
900°C,Vm
PRI (-)
Vm (cm3g-1)
Ca co-loaded (%)
0.03
0.02
0.01
0
0.25
0.2
0.15
0.1
0.05
0
0
0.5
1
1.5
(B)
850°C, SBET
850°C, Sm
900°C,SBET
900°C, Sm
SBET, Sm (m2 g-1)
Ca co-loaded (%)
350
250
150
50

Fig. 5.

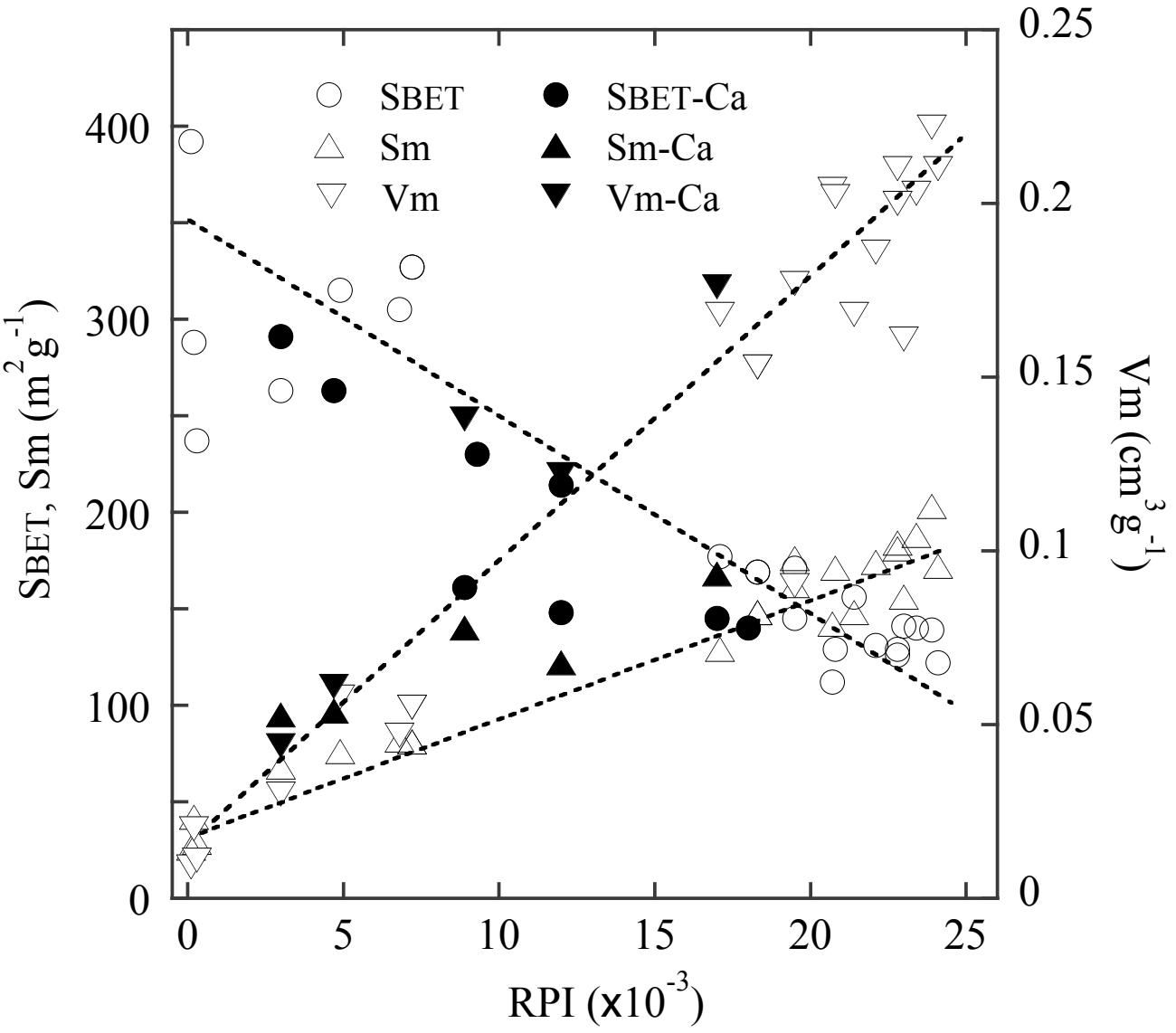
SBET
Sm
Vm
SBET-Ca
Sm-Ca
Vm-Ca
SBET, Sm (m2 g-1)
Vm (cm3 g-1)
RPI (x10-3)
0
100
200
300
400
0
0.05
0.1
0.15
0.2
0.25
0
5
10
15
20
25

Fig. 6.

Figure Captions:

Fig. 1. Reaction apparatus used for nickel-catalyzed carbonization

Fig. 2. XRD profiles of chars obtained from (A) Ni 1%-, (B) Ni 2%-, and (C) Ni4%-woods by carbonizations at 800, 850, and 900°C

Fig. 3. Nitrogen adsorption and desorption isotherms of (A) 800-, 850-, and 900°C-chars obtained from Ni2%-wood and (B) 900°C-chars obtained from Ni 1%-, Ni 2%-, and Ni 4%-woods

Fig. 4. Pore size distribution for (A) 800-, 850-, and 900°C-chars obtained from Ni2%-wood and (B) 900°C-chars obtained from Ni 1%-, Ni 2%-, and Ni 4%-woods

Fig. 5. Changes of (A) RPI and Vm and (B) S_{BET} and Sm with calcium co-loading for Ni-chars obtained by 850- and 900°C-carbonizations RPI, Vm, S_{BET}, and Sm; See the text

Fig. 6. Relation of S_{BET}, Sm, and Vm with RPI

Table 1. Yield and properties of none- and three kinds of Ni-chars obtained by carbonization at 800, 850, and 900°C.

Nickel loaded	Carbonization Temp. (°C)	Yield[a] (%)	*Lc*[b] (nm)	*d*002[c] (nm)	RPI[d] (x 10^{-3})	S_{BET}[e] (m^2/g)	Sm[f] (m^2/g)	Vm[g] (cm^3/g)	Rv[h] (%)
None	800	24.1	<1.0	---	---	392	26	0.009	13
	850	23.8	<1.0	---	---	288	42	0.020	48
	900	23.8	<1.0	---	---	237	29	0.011	16
1%	800	25.6	9.0	0.342	7.2	327	81	0.055	68
	850	25.5	9.6	0.341	18.3	169	148	0.153	90
	900	25.3	10.1	0.341	23.0	141	156	0.161	77
2%	800	26.0	7.9	0.341	4.9	315	76	0.058	77
	850	25.8	9.8	0.342	19.5	171	162	0.177	79
	900	25.5	10.1	0.342	23.4	140	188	0.203	71
4%	800	27.9	6.3	0.342	3.0	263	68	0.030	52
	850	27.6	9.1	0.342	17.1	177	129	0.168	83
	900	26.7	9.5	0.341	20.7	112	142	0.204	86

[a]Dry ash-free, additives-free basis [b]Average crystallite size of carbon indicating the thickness of the layer
[c]The spacing of the plane at (002) [d]Relative peak index, see the text [e]BET surface area [f]BJH surface area
[g]BJH mesopore volume [h]The ratio of Vm to Vt (total pore volume) used as the selectivity of mesoporosity

Table 2. Influence of helium flow, heating rate, and holding time on the relevant properties of Ni-chars obtained by 900°C-carbonization with 2% nickel.

Variables		*Lc*[a] (nm)	RPI[b] (x 10^{-3})	S_{BET}[c] (m^2/g)	Sm[d] (m^2/g)	Vm[e] (cm^3/g)	Va[f] (cm^3/g)	Vt[g] (cm^3/g)	Rv[h] (%)
Helium flow ($mlSTPcm^{-2}min^{-1}$)	5.8	9.9	20.8	129	171	0.202	0.103	0.309	65
	11.6	10.3	22.8	126	184	0.210	0.105	0.316	66
	23.2	10.1	23.4	140	188	0.203	0.084	0.287	71
	46.4	8.5	21.4	156	148	0.168	0.021	0.187	90
Heating rate ($°Cmin^{-1}$)	5	9.5	22.1	131	174	0.186	0.062	0.248	75
	10	10.1	23.4	140	188	0.203	0.084	0.287	71
	20	9.8	22.8	129	181	0.200	0.090	0.290	69
Holding time (min)	0	9.3	6.8	305	82	0.047	0.087	0.147[i]	32
	30	10.1	19.5	145	176	0.090	0.084	0174	52
	60	10.1	23.4	140	188	0.203	0.084	0.287	71
	90	11.0	23.9	139	203	0.222	0.104	0.326	68
	120	10.9	24.1	122	172	0.210	0.125	0.335	63

[a, b, c, d, e, h]See Table 1 [f]BJH macropore volume [g]BJH total pore volume = Vi(BJH micropore volume) +Vm +Va

[i]Vi was 0.013 cm^3/g, whereas it was < 0.001 cm^3/g for other specimens